Inorg. Chem. **2005**, *44*, 2012–2017

H-Bonding Interactions and Control of Thiolate Nucleophilicity and Specificity in Model Complexes of Zinc Metalloproteins

Jennifer N. Smith,[†] Justin T. Hoffman,[‡] Zahida Shirin,[†] and Carl J. Carrano*[,‡]

Departments of Chemistry and Biochemistry, San Diego State University, San Diego, California 92182-1030, and Texas State University, San Marcos, Texas 78666

Received September 30, 2004

It is shown in model complexes designed to mimic the binding site of zinc-thiolate proteins that a single hydrogen bond between an amide N–H and a Zn-coordinated thiolate reduces its reactivity toward electrophiles by up to 2 orders of magnitude. In addition, we show that a single N–H···S hydrogen bond is sufficient to achieve near 100% regiospecificity of reaction between a strong, and hence inherently indiscriminate, alkylating agent like trimethyloxonium tetraflouroborate and a single sulfur in a dithiolate construct. The importance of these results in understanding how systems such as the zinc fingers of the GATA family and the *E. coli* DNA repair protein Ada, which share the same pseudotetrahedral structure and tetracysteinyl ligation around the zinc, can fulfill such widely divergent (structural vs reactive) roles and how specificity of reaction in such multi-thiolate containing systems can be achieved is discussed.

Introduction

Thiolate coordination is an integral part of the coordination sphere of many of the hundreds of zinc metalloproteins known.[1] These sulfur rich zinc centers fulfill one of two basic functional roles, either as structural elements, as for example in the zinc fingers and some metalloregulatory proteins,[2,3] or as a reactive entity for alkyl group transfer as seen in the methionine synthesizing enzymes MetE and MetH of *E. coli* or in the DNA repair protein Ada.[4,5] However, a large number of unanswered questions remain about how the presence of the zinc modulates the reactivity of a thiolate anion. One such question is whether the reactive nucleophile in Zn(II)−S systems is a Zn(II)-bound thiolate or a dissociated thiolate anion. At issue is the nature of the nucleophile that leads to the transition state in this overall S_N2 reaction. In previous work, we and others have shown, at least for electroneutral complexes designed to mimic zinc thiolate protein coordination in nonpolar solvents, that the majority of the experimental evidence favors a Zn(II)-bound thiolate as the nucleophile.[6−9] Another, as yet, unanswered enigma is how two systems with essentially identical structure and ligation (compare for example the zinc fingers of the GATA family and the DNA repair protein Ada which both share the same pseudotetrahedral structure and CCCC ligation around the zinc) can fulfill widely divergent roles. In the latter case, the zinc thiolate functions as a reactive nucleophile that removes a methyl group from the phosphotriester backbone of alkylation damaged DNA while in the former case any such reactivity would be detrimental to its purely structural role. A related question requiring an answer is how, in a thiol rich construct such as that found in the Ada protein, is one specific zinc thiolate bond made to be reactive (cys 38 in this particular case) despite the similar steric accessibility of several such bonds.[5] Since it is well-known that the zinc-thiolate centers in the zinc fingers are involved in extensive N−H···S hydrogen bond networks with backbone amides, it has been proposed that such interactions might be a controlling factor in regulating reactivity and specificity of such bonds.[10] Although a statistical analysis of many Zn−S

* To whom correspondence should be addressed. E-mail: carrano@sciences.sdsu.edu.
† Texas State University.
‡ San Diego State University.

(1) Lipscomb, W. N.; Straeter, N. *Chem. Rev.* **1996**, *96*, 2375.
(2) Berg, J. M.; Shi, Y. *Science* **1996**, *271*, 1081.
(3) Outten, C. E.; O'Halloran, T. V. *Science* **2001**, *292*, 2488.
(4) (a) Matthews, R. G.; Goulding, C. W. *Curr. Opin. Chem. Biol*. **1997**, *1*, 332−339. (b) Hightower, K. E.; Fierke, C. A. *Curr. Opin. Chem. Biol*. **1999**, *3*, 176−81.
(5) Sun, L. J.; Yim, C. K.; Verdine, G. L. *Biochemistry* **2001**, *40*, 11596.
(6) Hammes, B. S.; Warthen, C. R.; Crans, D. C.; Carrano, C. J. *J. Biol. Inorg. Chem*. **2000**, *6*, 82.
(7) Brand, U.; Rombach, M.; Seebacher, J.; Vahrenkamp, H. *Inorg. Chem*. **2001**, *40*, 6151−6157.
(8) Chiou, S. J.; Innocent, J.; Riordan, C. G.; Lam, K. C.; Liable-Sands, L.; Rheingold, A. L. *Inorg. Chem*. **2000**, *39*, 4347.
(9) Bridgewater, B. M.; Fillebeen, T.; Friesner, R. A.; Parkin, G. *J. Chem. Soc., Dalton Trans.* **2000**, 4494.

10.1021/ic048630f CCC: $30.25
Published on Web 02/15/2005

Chart 1

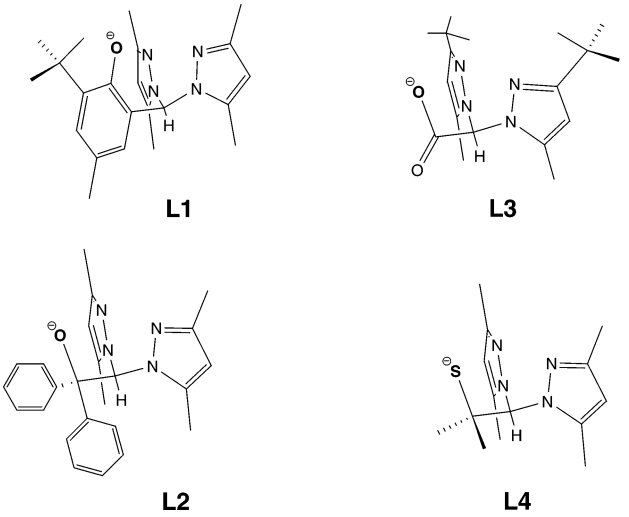

proteins pointed to a strong correlation between electrostatic screening of the core (predominantly by H-bonding interactions) and reactivity,[11] only recently using synthetic analogues has any experimental confirmation of this notion, or a determination of its magnitude, been reported.[12−14] In the present report, we study the alkylation of LZnSPh complexes designed to mimic the tetrahedral binding site found in all zinc thiolate proteins. In these complexes, the ligand L is one of a series of N_2X tripodal scorpionates designated L1−4 (Chart 1) containing phenolate oxygen, alkoxy oxygen, carboxylate oxygen, or thiolate sulfur donors, respectively, in the "X" position.[15−17] By substituting *o*-N-Ac-thiophenol (known to possess an internal hydrogen bond between the amide and the thiolate sulfur)[18−20] in place of thiophenol itself as the exogenous fourth ligand, we show that H-bonding can indeed control reactivity and that even a single such bond is sufficient to achieve specificity of reaction with a powerful, and hence inherently indiscriminate, electrophile. These results have a direct bearing on our understanding of these important metalloproteins. Portions of this work have already appeared in abbreviated form.[12]

(10) Meyers, L. C.; Verdine, G. L.; Wagner, G. *Biochemistry* **1993**, *32*, 14089.
(11) Maynard, A. T.; Covell, D. G. *J. Am. Chem. Soc*. **2001**, *123*, 1047.
(12) (a) Smith, J. N.; Shirin, S.; Carrano, C. J. *J. Am. Chem. Soc.* **2003**, *125* (4), 868−869. (b) For a recent summary of synthetic analogues relevant to the structure and function of zinc metalloproteins in general see: Parkin, G. *Chem. Rev.* **2004**, *104*, 699−767.
(13) Docrat, A.; Morlok, M. M.; Bridgewater, B. M.; Churchill, D. G.; Parkin, G. *Polyhedron* **2004**, *23*, 481−488.
(14) Chiou, S.; Riordan, C. G.; Rheingold, A. L. *Proc. Natl. Acad. Sci. U.S.A.* **2003**, *100*, 3695−3700.
(15) Hammes, B. S.; Carrano, C. J. *J. Chem. Soc., Dalton Trans*. **2000**, 3304.
(16) Hammes, B. S.; Kieber-Emmons, M. T.; Latizia, J. A.; Shirin, Z.; Carrano, C. J.; Rheingold, A. L. *Inorg. Chim. Acta* **2003**, *346*, 227−238.
(17) Hammes, B. S.; Carrano, C. J. *Inorg. Chem*. **1999**, *38*, 4593.
(18) Uyeama, N.; Okamura, T.; Nakamura, A. *J. Am. Chem. Soc*. **1992**, *114*, 8129.
(19) Ueyama, N.; Taniuchi, K.; Okamura, T.; Nakamura, A.; Maeda, H.; Emura, S. *Inorg. Chem.* **1996**, *35*, 1945.
(20) Okamura, T.; Takamizawa, S.; Ueyama, N.; Nakamura, A. *Inorg. Chem*. **1998**, *37*, 18−28.

Experimental Section

All syntheses were initially carried out under inert atmosphere, but subsequent workups were conducted in air. The reagents and solvents were purchased from commercial sources and used as received unless otherwise noted. EtOH and THF were distilled under argon over magnesium turnings/I_2 and Na/benzophenone, respectively. $CDCl_3$ was purchased from Aldrich and used as received. Ligands L1−4 and their corresponding methyl and thiophenolate zinc complexes were synthesized by literature methods.[15−17] 2,2′-Dithio-bis(*N*-phenylacetamide) and 2,2′-dithio-bis(*N*-phenyl-2,2,2-trifluoroacetamide) were prepared by reported procedures.[18−20]

[(L1)Zn(S-*o*-$CH_3CONHC_6H_4$)], 1. Solid $NaBH_4$ (0.02 g, 0.53 mmol) was added to a THF−ethanol (9:1, 25 mL) solution of 2,2′-dithiobis(*N*-phenylacetamide) (0.17 g, 0.51 mmol). The mixture was stirred at room temperature for about 2 h to give a clear solution, to which [(L1)$ZnCH_3$] (0.40 g, 0.89 mmol) was added. The resulting solution was stirred overnight, solvents were removed, and the solid was dried under reduced pressure. The resulting solid was redissolved in CH_2Cl_2, filtered through Celite, and crystallized by layering with hexane. Yield: 0.37 g (69%). Anal. Calcd for $C_{30}H_{37}N_5O_2S_1Zn\cdot(CH_2Cl_2)_{0.12}$: C, 59.57; H, 6.18; N, 11.53. Found: C, 59.59; H, 6.27; N, 11.43. FTIR (KBr), cm^{-1}: ν_{NH} 3324. FTIR (in CH_2Cl_2): ν_{NH} 3327. ^1H NMR ($CDCl_3$): δ 8.85 (s, 1H, N*H*), 8.33 (d, 1H, $J = 7.6$ Hz, S−Ar*H*), 7.80 (d, 1H, $J = 7.4$ Hz, S−Ar*H*), 7.06 (d, 1H, $J = 2.4$ Hz, Ar*H*), 7.02 (t, 1H, $J = 7.8$ Hz, S−Ar*H*), 6.90 (s, 1H, −C*H*−), 6.78 (t, 1H, $J = 7.8$ Hz, S−Ar*H*), 6.68 (d, 1H, $J = 2$ Hz, Ar*H*), 5.91 (s, 2H, Pz*H*), 2.46 (s, 6H, Pz−CH_3), 2.22 (s, 3H, S−ArCH_3), 2.20 (s, 6H, Pz−CH_3), 2.19 (s, 3H, ArCH_3),1.35 (s, 9H, −C(CH_3)$_3$). ^{13}C NMR ($CDCl_3$): δ 168.40, 163.02, 150.39, 142.69, 140.68, 138.43, 134.29, 130.34, 129.06, 124.57, 123.28, 120.66, 119.78, 119.19, 106.81, 73.50, 35.40, 29.33, 25.04, 20.40, 12.79, 11.62.

[(L1)Zn(S-*o*-$CF_3CONHC_6H_4$)], 2. Solid $NaBH_4$ (0.02 g, 0.53 mmol) was added to a THF-ethanol solution (9:1, 25 mL) of 2,2′-dithio-bis(*N*-phenyl-2,2,2-triflouroacetamide) (0.225 g, 0.51 mmol). The mixture was stirred at room temperature for about 2 h to give a clear solution, to which [(L1)$ZnCH_3$] (0.40 g, 0.89 mmol) was added. The resulting solution was stirred overnight, solvents removed, and the solid was dried under reduced pressure. The resulting solid was redissolved in CH_2Cl_2, filtered through Celite, and crystallized by layering with hexane. Yield 0.29 g (66%). FTIR (KBr), cm^{-1}: ν_{NH} 3247. FTIR (in CH_2Cl_2): ν_{NH} 3264. ^1H NMR ($CDCl_3$): δ 10.00 (s, 1H, N*H*), 8.34 (d, 1H, $J = 8$ Hz, S−Ar*H*), 7.89 (d, 1H, $J = 8$ Hz, S−Ar*H*), 7.10 (t, 1H, $J = 7.8$ Hz, S−Ar*H*), 7.05 (d, 1H, $J = 2.4$ Hz, Ar*H*), 6.94 (t, 1H, $J = 7.6$ Hz, S−Ar*H*), 6.90 (s, 1H, −C*H*−), 6.68 (d, 1H, $J = 2.0$ Hz, Ar*H*), 5.93 (s, 2H, Pz*H*), 2.46 (s, 6H, Pz−CH_3), 2.29 (s, 6H, Pz-CH_3), 2.18 (s, 3H, ArCH_3) 1.26 (s, 9H, −C(CH_3)$_3$). ^{13}C NMR ($CDCl_3$): δ 162.93, 150.37, 142.69, 140.78, 134.98, 130.40, 129.15, 125.28, 125.05, 120.81, 119.75, 119.46, 106.87, 73.53, 35.36, 29.20, 20.43, 12.92, 11.66.

[(L3)Zn(S-*o*-$CH_3CONHC_6H_4$)], 3. This complex was synthesized by the same method as described for **1**. Colorless crystals were obtained from CH_2Cl_2/diisopropyl ether solution in 60% yield. Anal. Calcd for $C_{26}H_{35}N_5O_3SZn\ (CH_2Cl_2)_{0.1}$: C, 54.85; H, 6.21; N, 12.25. Found: C, 54.91; H, 6.16; N, 11.98. FTIR (KBr), cm^{-1}: ν_{NH} 3307. FTIR (in CH_2Cl_2): ν_{NH} 3341. ^1H NMR ($CDCl_3$): δ 8.85 (s, 1H, N*H*), 8.26 (d, 1H, $J = 7.6$ Hz, S−Ar*H*), 7.72 (d, 1H, $J =$ 8 Hz, S−Ar*H*), 7.03 (t, 1H, $J = 8$ Hz, S−Ar*H*), 6.84 (t, 1H, $J =$ 7.6 Hz, S−Ar*H*), 6.60 (s, 1H, −C*H*−), 6.05 (s, 2H, Pz*H*), 2.45 (s, 6H, Pz−CH_3), 2.26 (s, 3H, S−ArCH_3),1.27 (s, 18H, Pz−(CH_3)$_3$). ^{13}C NMR ($CDCl_3$): δ 164.72, 141.53, 135.49, 125.85, 123.47, 119.66, 104.84, 67.68, 31.96, 30.23, 25.12, 11.25.

[(L2)Zn(S-*o*-$CH_3CONHC_6H_4$)], 4. The disulfide 2,2′-dithiobis-(*N*-phenylacetamide) (107 mg, 0.32 mmol) was reduced with potassium borohydride (17.4 mg, 0.32 mmol) in 50 mL of a 9:1 mixture of anhydrous THF−ethanol under inert atmosphere. The solution was allowed to stir overnight when [(L2)ZnCH_3] (250 mg, 0.54 mmol) was added to the solution. After stirring for 1 h, the solution was reduced to dryness and brought into the drybox. The crude product was dissolved in anhydrous CH_2Cl_2, and filtered through a pad of Celite. The resulting clear solution was reduced to dryness to yield 205 mg (62% yield) of white crystalline product. X-ray quality crystals of [(L2)Zn(S-*o*-$CH_3CONHC_6H_4$)] were produced by layering a concentrated CH_2Cl_2 solution of the complex with hexanes. Anal. Calcd (Found) for [(L2)Zn(S-*o*-$CH_3CONHC_6H_4$)], $C_{32}H_{33}N_5O_2SZn\cdot(CH_2Cl_2)_2\cdot H_2O$: C, 50.73 (50.39); H, 4.88 (4.69); N, 8.70 (8.61). ^{1}H NMR ($CDCl_3$): δ 9.05 (s, 1 H, −N*H*−), 8.27 (d, 1 H, SAr*H*), 7.76 (d, 1 H, SAr*H*), 7.54 (dd, 4 H, Ar*H*), 7.19 (m, 4 H, Ar*H*), 7.15 (m, 2 H, Ar*H*), 7.04 (m, 1 H, SAr*H*), 6.84 (m, 1 H, SAr*H*), 6.60 (s, 1 H, −C*H*−), 5.67 (s, 2 H, Pz*H*), 2.22 (s, 3 H, Ar−CH_3), 2.03 (s, 6 H, Pz−CH_3), 2.00 (s, 6 H, Pz−CH_3). ^{13}C NMR ($CDCl_3$): δ 168.67, 149.78, 146.35, 141.27, 139.00, 134.45, 128.04, 126.97, 126.91, 126.85, 124.80, 123.39, 120.13, 105.68, 84.75, 70.96, 25.07, 12.65, 10.84.

[(L4)Zn(S-*o*-$CH_3CONHC_6H_4$)], 5. The complex was synthesized by the same method as described for **1**. Colorless crystals were obtained in 65% yield. Anal. Calcd for $C_{22}H_{29}N_5OS_2Zn$: C, 51.91; H, 5.74; N, 13.76. Found: C, 51.97; H, 5.72; N, 13.68. FTIR (KBr), cm^{-1}: ν_{NH} 3324. FTIR (in CH_2Cl_2): ν_{NH} 3326. ^{1}H NMR ($CDCl_3$) δ 8.89 (s, 1H, N*H*), 8.32 (d, 1H, J = 8.4 Hz, S−Ar*H*), 7.46 (d, 1H, J = 7.6 Hz, S−Ar*H*), 6.99 (t, 1H, J = 7.8 Hz, S−Ar*H*), 6.77 (t, 1H, J = 8 Hz, S−Ar*H*), 5.98 (s, 1H, −C*H*−), 5.96 (s, 2H, Pz*H*), 2.39 (s, 6H, Pz−CH_3), 2.27 (s, 6H, Pz−CH_3), 2.23 (s, 3H, S−ArCH_3), 1.35 (s, 6H, −C(CH_3)$_2$). ^{13}C NMR ($CDCl_3$): δ 149.98, 141.03, 133.91, 124.64, 123.19, 119.02, 106.52, 72.95, 48.26, 33.73, 25.16, 12.96, 11.42.

[(L4SCH_3)Zn(S-*o*-$CH_3CONHC_6H_4$)], 6. A CH_3CN solution of $(CH_3)_3OBF_4$ (0.08 g, 0.54 mmol) was added dropwise into the solution of [(L4)Zn(S-*o*-$CH_3CONHC_6H_4$)] (0.28 g, 0.55 mmol) in 25 mL of CH_3CN. The resulting reaction mixture was stirred for 2 h, filtered, and crystallized by slow diffusion of diethyl ether. Yield 0.27 g (80%). Anal. Calcd for $C_{23}H_{32}N_5OS_2BF_4Zn$: C, 45.22; H, 5.28; N, 11.46. Found: C, 44.94; H, 5.01; N, 11.62. FTIR (KBr), cm^{-1}: ν_{NH} 3327. ^{1}H NMR (CD_3CN): δ 9.18 (s, 1H, N*H*), 7.67 (d, 1H, J = 6.8 Hz, S−Ar*H*), 7.52 (d, 1H, J = 7.6 Hz, S−Ar*H*), 7.14 (t, 1H, J = 7.6 Hz, S−Ar*H*), 7.07 (t, 1H, J = 7.2 Hz, S−Ar*H*), 6.21 (s, 2H, Pz*H*), 6.15 (s, 1H, −C*H*−), 2.45 (s, 6H, Pz−CH_3), 2.12 (s, 6H, Pz−CH_3), 2.08 (s, 3H, S−ArCH_3), 1.67 (s, 3H, SCH_3), 1.17 (s, 6H, −C(CH_3)$_2$). ^{13}C NMR ($CDCl_3$): δ 152.4, 145.48, 136.66, 125.86, 125.40, 123.42, 107.28, 70.56, 51.42, 25.04, 23.44, 13.11, 12.17, 11.02.

X-ray Crystallography. Crystals of complexes **1**−**6** were sealed in thin-walled quartz capillaries or nylon loops (Hampton Research), and mounted on either a Siemens P4, Nonius Kappa CCD, or Bruker X8 APEX CCD diffractometer. The structures were solved using direct methods or via the Patterson function, completed by subsequent difference Fourier syntheses, and refined by full-matrix least-squares procedures on F^2. All non-hydrogen atoms were refined with anisotropic displacement coefficients and treated as idealized contributions using a riding model except where noted. All software and sources of the scattering factors are contained in the SHELXTL 6.0 program library (G. Sheldrick, Siemens XRD, Madison, WI). Crystallographic data collection parameters are given in Table 1 while selected bond lengths and angles for complexes **1**−**5** are shown in Table 2 and for **6** in Table 3. The ORTEP diagram for [(L1)Zn(NAcSPh)] is shown in Figure 1, for [(L4)-Zn(NAcSPh)], it is in Figure 2, for [(L3)Zn(NAcSPh)], it is in Figure 3, for [(L2)Zn(S-*o*-$CH_3CONHC_6H_4$)], it is in Figure 4, and for [(L4SCH_3)Zn(NAcSPh)], it is in Figure 5.

Kinetic Experiments. All experiments were performed under pseudo-first-order conditions with the alkylating agent in 10-fold excess as previously described.[6] In a typical experiment, 1.8×10^{-5} mol of the metal complex was dissolved in 1 mL of solvent to give an 18 mM solution. In a few cases, reactions were also run at 5 or 10 mM in metal complex. The solution of the metal complex was then transferred to a NMR tube, and the alkylating agent added via a gastight syringe. The NMR tube was then sealed with a septum. The reactions were monitored by ^{1}H NMR spectroscopy at 25 °C. The kinetic data were least-squares fit to a single exponential to determine the pseudo-first-order rate constant. Data analysis was performed using Sigmaplot 8.0 (Jandel Scientific) software.

Results and Discussion

Synthesis and Structure. We have previously used the reaction of LZnSPh complexes with CH_3I to model the reaction of Zn−S bonds with an electrophile in solution.[6] To mimic the presence of an amide hydrogen to sulfur H-bond, we have utilized *o*-N-Ac-thiophenol in place of thiophenol as the exogenous fourth ligand. *o*-N-Ac-thiophenol and its derivatives are known to possess an internal hydrogen bond between the amide and the thiolate sulfur, and extensive studies by Nakamura et al. have demonstrated the profound effects such bonds can have on redox potentials and other thermodynamic properties in models for Fe−S and molybdopterin proteins.[18−20] In our case, the desired complexes were readily prepared by borohydride reduction of the disulfide of the appropriate *o*-*N*-acetylated thiophenol followed by in situ reaction with [LZnCH_3] in THF−ethanol. We have isolated and completely characterized the [LZn(*o*-N-Ac-thiophenol)] complexes for the L1−4 heteroscorpionate ligands. For comparative purposes, we have also isolated and structurally characterized [(L1)Zn(*o*-N-trifluoromethylacetyl-thiophenol)]. As can be seen in the crystal structures of both the L1 and L4 complexes, an internal H-bond of the same type and nearly the same geometrical parameters as those described by Nakamura is present.[18−20] These have H···S "bond" distances between 2.36 and 2.45 Å and N−H···S angles between 113° and 117°. The distance between the N_{amide}−H and the heteroatom of the heteroscorpionate ligand is greater than 5 Å in all these cases as the amido group is oriented to maximize the hydrogen bonding interaction with the thiolate sulfur. However, an examination of the structures of the L2 and L3 complexes reveals a different story. In the case of the L3 complex, **3**, the *o*-N-Ac-thiophenol is now oriented in such a way as to maximize the H-bonding not with the thiolate sulfur but with the carboxylate oxygen of the heteroscorpionate ligand. Indeed, the N−H···$O_{carboxylate}$ distance is very short (1.99 Å), and the N−H···O angle is nearly linear (172°), both of which are suggestive of a very strong internal hydrogen bond. This results in a weak interaction with the thiolate sulfur as reflected in the long N−H···S (2.99 Å) "bond" and acute N−H···S angle. The situation with the L2 alkoxy ligand

Table 1. Summary of Crystallographic Data and Parameters for [L1ZnS-*o*-$CH_3CONHC_6H_4$·CH_2Cl_2] (**1**), [L1ZnS-*o*-$CF_3CONHC_6H_4$] (**2**), [L3ZnS-*o*-$CH_3CONHC_6H_4$] (**3**), [L2ZnS-*o*-$CH_3CONHC_6H_4$] (**4**), [L4ZnS-*o*-$CH_3CONHC_6H_4$] (**5**), and [L4SCH_3Zn S-*o*-$CH_3CONHC_6H_4$] (**6**)

	1	**2**	**3**	**4**	**5**	**6**
molecular formula	$C_{31}H_{39}Cl_2N_5O_2SZn$	$C_{30}H_{34}F_3N_5O_2SZn$	$C_{26}H_{35}N_5O_3SZn$	$C_{32}H_{33}N_5O_2SZn$	$C_{22}H_{29}N_5OS_2Zn$	$C_{23}H_{32}BF_4N_5OS_2Zn$
fw	682	651.05	562.95	617.09	508.99	610.84
temp (K)	293(2)	293(2)	153	273(2)	293(2)	293(2)
cryst syst	monoclinic	triclinic	monoclinic	monoclinic	monoclinic	monoclinic
space group	$P2_1/c$	$P\bar{1}$	$P2_1/c$	$P2_1/c$	$P2_1/c$	$P2_1/n$
cell constants						
a (Å)	10.915(3)	13.793(3)	17.912(2)	34.5132(9)	10.356(2)	13.780(2)
b (Å)	13.024(5)	15.131(5)	9.839(10)	8.4159(2)	13.930(3)	13.386(2)
c (Å)	23.832(6)	17.356(9)	17.074(2)	20.7128(5)	16.680(3)	15.197(2)
α (deg)	90	90	90	90	90	90
β (deg)	102.27	93.38(3)	111.6520(10)	95.0900(10)	92.29(3)	91.05
γ (deg)	90	114.84(2)	90	90	90	90
Z	4	4	4	6	4	4
V (Å^3)	3311(2)	3279(2)	2796.87(5)	5992.5(3)	2404.3(8)	2802.8(7)
abs coeff, μ_{calc} (mm^{-1})	1.002	0.863	0.987	1.353	1.219	1.078
δ_{cal} (g/cm^3)	1.368	1.319	1.316	1.436	1.406	1.448
F(000)	1424	1352	1148	2676	1064	1264
cryst dimens (mm^3)	0.5 × 0.2 × 0.3	0.8 × 0.6 × 0.2	0.4 × 0.08 × 0.07	0.2 × 0.2 × 0.4	0.29 × 0.13 × 0.12	0.4 × 0.4 × 0.4
radiation	Mo Kα (λ = 0.71073 Å)	Mo Kα (λ = 0.71073 Å)	Mo Kα (λ = 0.71073 Å)	Mo Kα (λ = 0.71073 Å)	Mo Kα (λ = 0.71073 Å)	Mo Kα (λ = 0.71073 Å)
h,k,l ranges colled	0 → 12, −15 → 0, −28 → 27b	−16 → 0, −14 → 16, −18 → 18	−25 → 25, −13 → 13, −22 → 23	−36 → 36, −8 → 8, −22 → 22	−13 → 13, −18 → 18, −21 → 21	0 → 16, 0 → 15, −18 → 18
θ range (deg)	1.79−25.01	2.06−23.03	2.93−27.50	1.78−22.41	3.08−27.50	1.98−25.00
no. reflns colled	6096	9785	12135	67632	10381	5051
no. unique reflns	5782	9051	6392	7699	5465	4845
no. params	379	757	337	739	283	362
data/param ratio	15.12	11.94	18.89	10.42	19.31	13.38
refinement method	*a*	*a*	*a*	*a*	*a*	*a*
$R(F)^b$	0.0563	0.0692	0.0476	0.0387	0.0407	0.0748
$R_w(F^2)^c$	0.1446	0.1518	0.1136	0.0982	0.0943	0.1156
GOFw^d	1.031	1.028	1.071	0.995	1	1.031
largest diff peak and hole (e/Å^3)	0.85 and −0.79	0.59 and −0.45	0.63 and −0.63	0.468 and −0.257	0.522 and −0.393	0.41 and −0.36

[a] Full-matrix least-squares of F^2. [b] $R = [\sum|\Delta F|/\sum|F_o|]$. [c] $R_w = [\sum w(\Delta F)^2/\sum wF_o^2]$. [d] Goodness of fit on F^2.

Table 2. Selected Bond Lengths (Å) and Angles (deg) for **1**−**5**

	1	**2**	**3**	**4**	**5**
Zn−N1	2.037(3)	2.031(7)	2.050(2)	2.064(3)	2.054(2)
Zn−N3	2.023(3)	2.014(7)	2.058(2)	2.041(3)	2.077(2)
Zn−X	1.887(3)	1.908(6)	2.002(2)	1.910(2)	2.257(1)
Zn−S1	2.2201(13)	2.241(3)	2.2219(8)	2.223(1)	2.2482(9)
N1−Zn−N3	88.92(13)	90.6(3)	88.80(10)	89.16(12)	85.81(9)
N1−Zn−X	97.91(14)	95.9(3)	91.52(9)	93.58(10)	99.00(7)
N1−Zn−S1	122.92(10)	124.3(2)	124.48(7)	123.15(9)	116.31(7)
N3−Zn−X	101.50(14)	100.8(3)	91.63(9)	91.35(11)	97.04(7)
N3−Zn−S1	117.83(10)	117.1(2)	136.25(7)	131.07(9)	116.73(7)
X−Zn−S1	121.27(10)	121.6(2)	112.50(6)	118.59(8)	131.45(3)
S1···H_{amide}	2.412(*)	2.450(*)	2.994(*)	2.865(*)	2.358(*)
X···H_{amide}			1.992(*)	2.390(*)	
N5−H···S1	117.2(*)	117.0(*)	93.5(*)	95.5(*)	113.0(*)
N5−H···X			172.0(*)	135.0(*)	

Table 3. Selected Bond Lengths (Å) and Angles (deg) for **6**

Zn−N1	2.047(6)
Zn−N3	2.045(7)
Zn−S1	2.773(3)
Zn−S2	2.254(2)
Zn−O1	2.102(6)
N1−Zn−N3	91.8(3)
N1−Zn−S1	79.9(2)
N1−Zn−S2	131.7(2)
N1−Zn−O1	98.3(2)
N3−Zn−S1	82.6(2)
N3−Zn−S2	132.9(2)
N3−Zn−O1	96.2(2)
S1−Zn−S2	87.91(9)
S1−Zn−O1	177.8(2)
S2−Zn−O1	94.2(2)

complex is between the two extremes in that the *o*-N-Ac-thiophenol is oriented in such a way as to allow a bifurcated H-bonding interaction with both the thiolate sulfur and the alkoxy oxygen. However, the stronger interaction is clearly with the heteroscorpionate ligand alkoxy oxygen as indicated by its shorter (2.39 vs 2.87 Å) and more linear (135° vs 95°) N−H···X interaction.

Effects of Hydrogen Bonding on Kinetics of Thiolate Alkylation. To determine the effects that this internal H-bond has on the reactivity of the zinc thiolate, we have compared the kinetics of reaction between **1** and its non-hydrogen-bond-containing analogue in $CDCl_3$ with CH_3I at 25 °C. The results (Table 4) show that the presence of a single H-bond is sufficient to reduce the reactivity of the Zn−S bond toward the electrophile by approximately 2 orders of magnitude. Thus, we were initially greatly surprised when repeating this experiment using the L3 complex **3** and its non-H-bonding analogue, that the effect was now greatly reduced (reactivity reduced only by a factor of 7). A solution to this puzzle became evident however from an examination of the crystal structure of **3** (vide supra) which clearly revealed that the H-bond formed in this case was with the carboxylate oxygen of the scorpionate ligand and *not* the thiolate sulfur. This provides a definitive and sensitive test to show that it is the H-bond itself rather than any peripheral electronic or steric effect of the N-acetyl group that controls the reactivity of

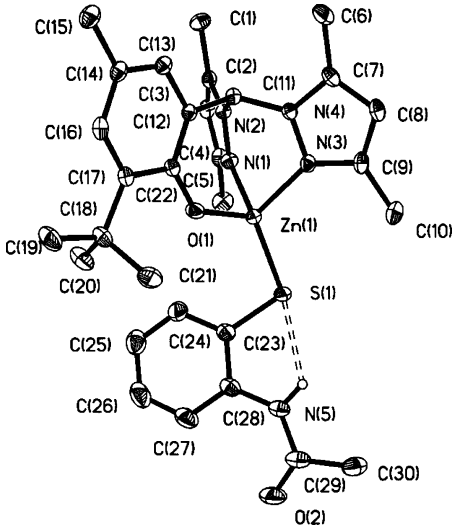

Figure 1. ORTEP diagram with 40% thermal ellipsoids of [(L1)Zn-(NAcSPh)] showing complete atomic labeling.

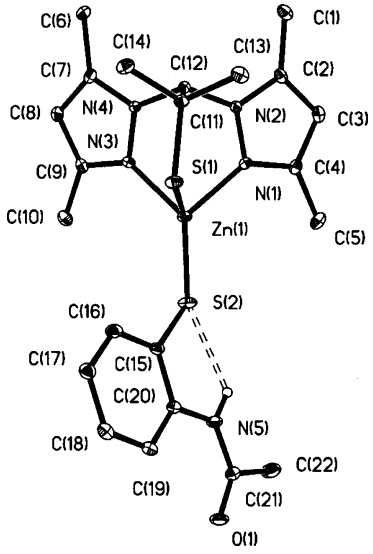

Figure 2. ORTEP diagram with 40% thermal ellipsoids of [(L4)Zn-(NAcSPh)] showing complete atomic labeling.

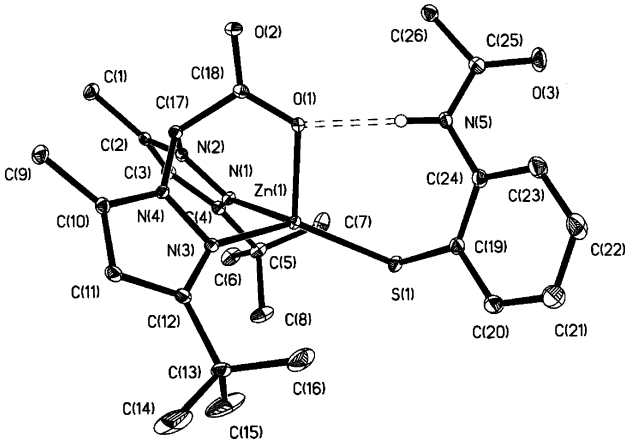

Figure 3. ORTEP diagram with 40% thermal ellipsoids of[(L3)Zn-(NAcSPh)] showing complete atomic labeling.

the thiolate. The relative decrease in reactivity between [(L2)-Zn(SPh)] and [(L2)Zn(S-*o*-$CH_3CONHC_6H_4$)] is also only approximately 1 order of magnitude, consistent with an

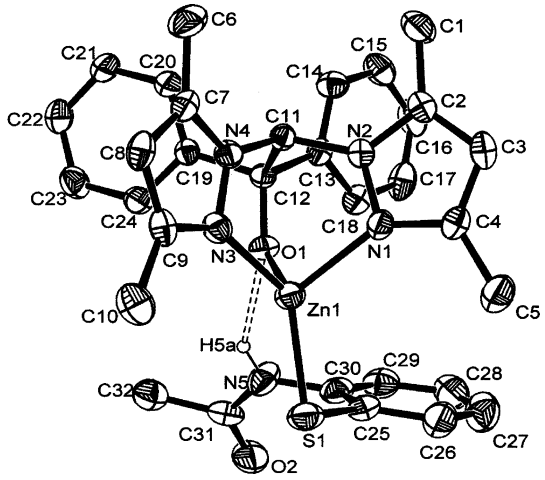

Figure 4. ORTEP diagram with 50% thermal ellipsoids of[(L2)Zn-(NAcSPh)] showing complete atomic labeling.

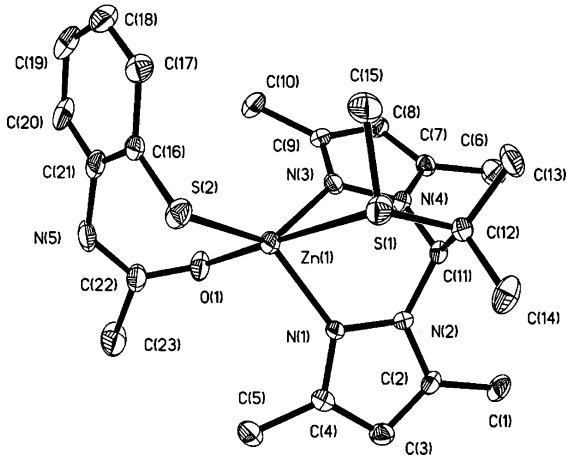

Figure 5. ORTEP diagram with 50% thermal ellipsoids of[($L4SCH_3$)Zn-(NAcSPh)] showing complete atomic labeling.

Table 4. Pseudo-First-Order Rate Constants (s^{-1}) Determined by ^1H NMR for Reaction of the Listed Compounds (18 mM) with Methyl Iodide (180 mM) at 25 °C

compd	chloroform av rate ($\times 10^{-4}$)	acetonitrile av rate ($\times 10^{-4}$)
[(L4)ZnI]	3.12(8)	27(6)
[(L1)Zn(SPh)]	3.53(5)	14.2(3)
[(L1)Zn(NAcSPh)]	0.017(1)	0.41(5)
[(L1)Zn($NCOCF_3$SPh)]	0.026(2)	1.3(4)
[(L3)Zn(SPh)]	0.028(2)	0.14(4)
[(L3)Zn(NAcSPh)]	0.004(4)	0.059(1)
[(L2)Zn(SPh)]	2.0(1)	nd
[(L2)Zn(NAcSPh)]	0.23(6)	nd

internal H-bond that is more with the alkoxy oxygen of the ligand than with the thiolate sulfur. This was confirmed again by a crystal structure analysis (Figure 4).

If H-bonding can control the reactivity of the Zn-thiolate with electrophiles, then it can in principle also provide a means to generate specificity. To test the degree of such specificity we designed a model system, [(L4)Zn(*o*-N-Ac-thiophenol)], **5**, which contains two thiolates, one involved in H-bonding and the other not. Despite the differing nature of the thiols (i.e., aliphatic vs aromatic), in the absence of H-bonding effects the thiophenol and heteroscorpionate thiolate sulfurs react at similar rates (Table 4). To provide a strict test of the degree of selectivity, we deliberately chose

the strong and hence inherently indiscriminate alkylating agent, trimethyloxonium tetrafluoroborate. The result was in many ways remarkable with only the L4 thiolate sulfur being alkylated to give the mono-thioether product **6**. Even with a single H-bond, the specificity was near 100% (we found no trace of the alternative methylated product).

Coordination of the Thioether. Another aspect of certain enzymatic reactions mimicked by our model system is the fact that, in many of the former, the thioether produced in the alkyl transfer remains coordinated to the zinc. Thioether coordination has been unequivocally demonstrated for the Ada protein, and spectroscopic evidence consistent with this has been presented in at least one other case.[21] The coordinated thiolate in a series of zinc complexes of our tripodal, N_2S ligand (L4) has been methylated in solution, and the coordination properties of the resulting thioether have been examined.[22,23] This system models the reactivity of zinc containing enzymes involved in alkyl group transfers. While it is clear that neutral thioethers cannot, in general, compete with anionic ligands, it is equally clear that a special, sterically restricted, protein environment is not necessary to support neutral thioether coordination. Thus, the thioether in **6** is weakly bound to the Zn as indicated by its position and its long (2.77 Å) "bond" length. The acetyl-carbonyl serves to provide the fourth strong ligand donor.

Biological Implications. What insight into the functioning of thio-rich zinc cores in metalloproteins can be gleaned from this work? First, this work supports the notion that zinc-thiolate cores, which are predicted to be inherently reactive constructs, can be deactivated by the presence of hydrogen bonds in complete accord with a recent detailed statistical analysis.[11] Thus, the unreactive CCCC cores found in the GATA zinc fingers are found to be more electrostatically screened than average while the correspondingly reactive CCCC core of Ada is less screened than average.[11] Second, it suggests that the presence of hydrogen bonds between the accessible but unreactive cys 69 or 42 and their absence at cys 38 could be the means by which the well-known regiospecifity of Ada is maintained. Gratifyingly, the most recent NMR structure of an active fragment of the Ada protein, N-Ada10, is reported to contain characteristic H-bonds to the ligand sulfur atoms for cys-69 and 42 and but not to the reactive cys-38.[24] In this regard, it is notable that those amide protons on residues near the sulfur atoms other than cys-38 exchange very slowly as expected for those engaged in hydrogen bond interactions.[25]

In conclusion, we have shown that even a single hydrogen bond to a thiolate sulfur is sufficient to drastically reduce its nucleophilicity. Thus, nature can use this mechanism to modulate the reactivity of a zinc-thiolate construct so that it can be used for either structural or reactive purposes. In addition, such hydrogen bonding provides another means to generate the exquisite specificity seen in reactive biomolecules of this type.

Acknowledgment. This work was supported by Grants CHE-02023535 and CHE-0313865 from the NSF. The NSF-MRI program Grant CHE-0320848 is acknowledged for support of the X-ray diffraction facilities at San Diego State University. The authors thank Dr. Vincent Lynch, University of Texas at Austin, for data collection on compounds **2** and **3** and Dr. Brian Hammes, St. Joseph's University, for a sample of ligand L3.

Supporting Information Available: X-ray crystallographic files (in CIF format) for **2** and **4** and ORTEP diagram for **2**. This material is available free of charge via the Internet at http://pubs.acs.org. X-ray crystallographic files (in CIF format) for **1**, **3**, **5**, and **6** can be obtained from the Supporting Information available for ref 12.

IC048630F

(21) Huang, C.; Casey, P. J.; Fierke, C. A. *J. Biol. Chem*. **1997**, *272*, 20−23.
(22) Hammes, B. S.; Carrano, C. J. *Inorg. Chem*. **2001**, *40*, 919−927.
(23) Hammes, B. S.; Carrano, C. J. *J. Chem. Soc*., *Chem Commun*. **2000**, 1635.
(24) (a) Lin, Y.; Doetsch, V.; Winter, T.; Peariso, K.; Myers, L. C.; Penner-Hahn, J. E.; Verdine, G. L.; Wagner, G. *Biochemistry* **2001**, *40*, 4261. (b) Personal communication.
(25) Habezettl, J.; Myers, C. M.; Yuan, F.; Verdine, G. L.; Wagner, G. *Biochemistry* **1996**, *35*, 9335−9348.